

Angular momentum during unexpected multidirectional perturbations delivered while walking

Dario Martelli, Vito Monaco, Lorenzo Bassi Luciani and Silvestro Micera, *Senior Member, IEEE*

Abstract—This study investigated the hypothesis that the coupled contribution of all body segments to the whole body response during both walking and managing unexpected perturbations is characterized by similar features which do not depend on the laterality (i.e., right versus left sides), but can be influenced by the direction (e.g., north, east, south, etc.) of the perturbation. The whole body angular momentum was estimated as summation of segmental angular momenta, while fifteen young adults managed ten unexpected unilateral perturbations during walking. Then, the Principal Component Analysis was used to extract primitive features describing inter-segment coordination. Results showed that inter-segment coupling was similar even though the reactive response to the perturbations elicited more consistent motor schemes across body segments than during walking, especially in the frontal plane. The direction of the perturbation significantly ($p < 0.05$) affected angular momentum regulation documenting the attitude of the CNS to interpret multiple sensory inputs in order to produce context-dependent reactive responses. With respect to the side, results highlighted anisotropic features of the elicited motor schemes which seemed to depend on subjects' dominance. Finally, results confirm that the coordination of upper and lower body segments is synergistically achieved strengthening the hypothesis that it may result from common neural pathways.

Index Terms—Angular momentum, perturbation, walking, inter-limb coordination, balance control.

I. INTRODUCTION

MANY research groups have provided experimental and theoretical descriptions of incipient fall biomechanics underlining high coordination of lower limbs while reactively managing stepping [1, 2], slipping [3-5] or tripping [6, 7]. For

Manuscript received November 28, 2012. This work was supported by the European Commission 7th FP, projects: CLONS “CLOsed-loop Neural prostheses for vestibular disorders” (GA 225929); CYBERLEGS “The CYBERnetic LowEr-Limb CoGnitive Ortho-prosthesis” (ICT 287894); I-DONT-FALL “Integrated prevention and Detection sOlutioNs Tailored to the population and Risk Factors associated with FALLs” (GA 297225).

Monaco V. (corresponding author; P.zza Martiri della Libertà, 33, 56127 Pisa, Italy; phone: +39 050.883007; fax: +39 050.883101; e-mail: v.monaco@sssup.it), Martelli D. (e-mail: d.martelli@sssup.it), Bassi Luciani L. (e-mail: l.bassiluciani@sssup.it) and Micera S. (e-mail: micera@sssup.it) are with The BioRobotics Institute, Scuola Superiore Sant'Anna, Pisa (I).

Micera S., is also with the Translational Neural Engineering Laboratory, Center for Neuroprosthetics, Swiss Federal Institute of Technology, Lausanne (CH).

instance, during slipping, subjects utilize suitable strategies involving early onset of the double support, expansion of the base of support and, consequently, increased stability [5].

Upper limb reactions, occurring at latencies similar to those of the legs [8], also contribute to balance recovery by mainly shifting the whole body centre of mass and counteracting the angular momentum in the direction of the perturbation [5, 9-11]. These reactions give more time to recover balance, help to restore posture and may serve as a protective strategy.

The simultaneous coordination of upper and lower limb movements led previous authors to conclude that whole body response is elicited during a dynamic motor task to guarantee dynamical stability [5, 8, 10]. In this respect, the regulation of the Whole Body Angular Momentum (WBAM) during locomotion reflects the paired contribution of different body segments, by means of suitable and consistent coupling of their Segmental Angular Momenta (SAM) [12-14]. This coordinative strategy does not depend on speed [14], and represents a key variable to keep balance during multi-body dynamic motor tasks such that it is supposed to be highly regulated by the Central Nervous System (CNS) [12, 13].

In accordance with these findings, some authors argued that the coordinated movement of upper and lower limbs could come from common nervous structures [8, 10, 15]. In particular, they suggested that suitable nervous pathways may serve as a functional link between the arms and legs while maintaining stability during locomotion. These nervous structures would hence connect the pattern generators of upper and lower limbs in order to ensure that their contribution is suitably coupled while managing balance.

In order to provide strong support to this hypothesis, we investigated the biomechanics of the corrective reactions of all body segments in response to unexpected and multidirectional slipping perturbations. We specifically hypothesized that the coupled contribution of all body segments to the whole body response during intrinsically different and unstable motor tasks – trained walking versus unexpected perturbation – is characterized by similar features. Moreover, we hypothesized that inter-limb coordination was similar with respect to the laterality (i.e., right versus left sides) of the perturbation, due to the symmetry of the motor tasks, but could show discrepancies across the direction (i.e., paired NL/NR, NW/NE, W/E, SW/SE, and SL/SR; see Material and

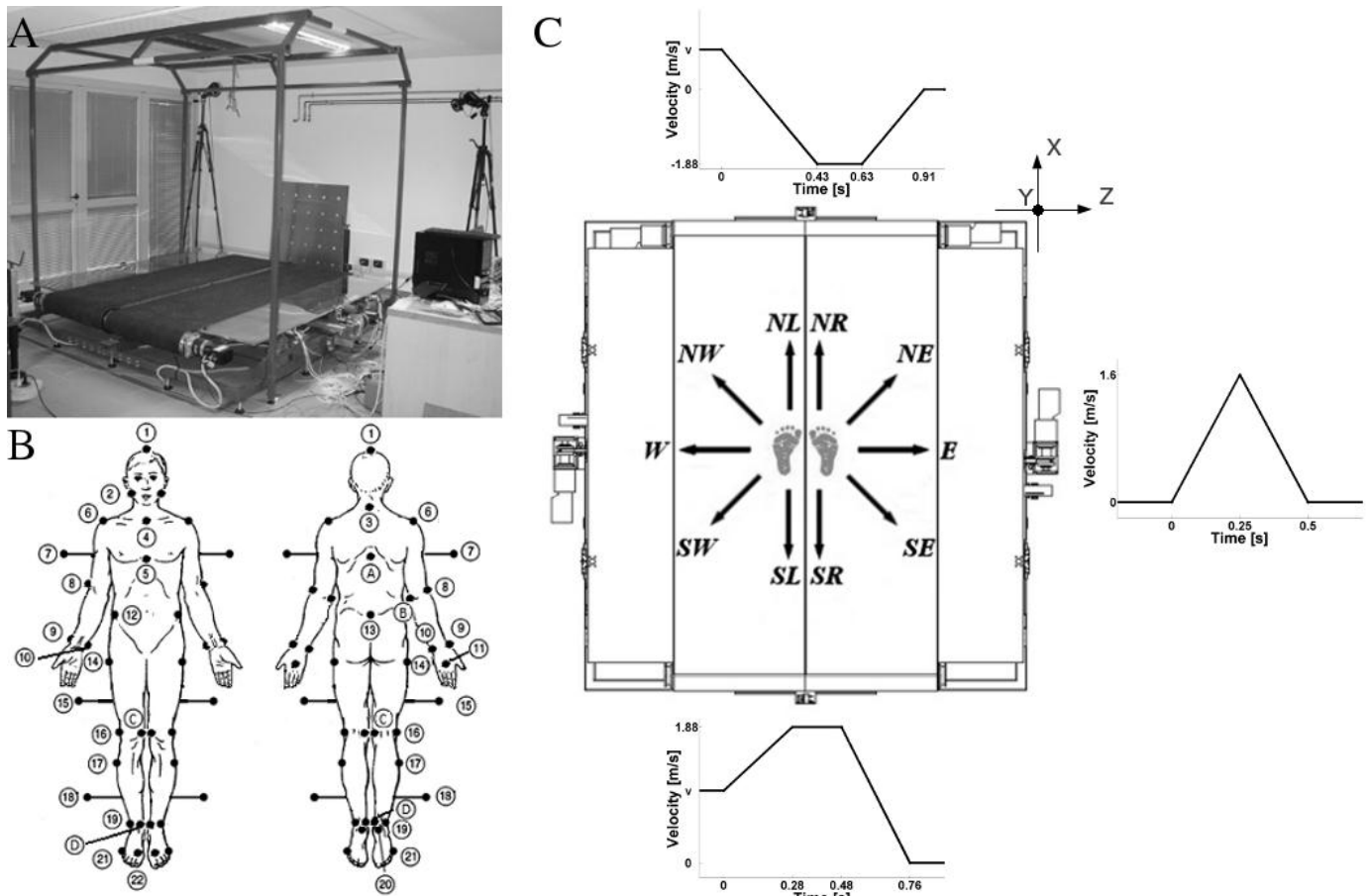


Fig. 1. **A:** The picture shows SENLY. **B:** Marker set. Markers were mounted bilaterally (the figure shows only those on the right side of the body to make reading easier) on: vertex (1), left and right gonions (2), for the head; C7 vertebrae (3), clavicle (4), sternum (5), and acromions (6), for the upper trunk; lateral epicondyle of the humeri (8), radial styloids (9), ulnar styloids (10), third metacarpal bones (11) and additional markers rigidly attached to wands over the mid-humeri (7), for both arms; anterior superior iliac spines (12) and sacrum (13), for the pelvis; prominence of the greater trochanters external surface (14), lateral epicondyle of the femurs (16), heads of fibula (17), lateral malleolus (19), calcaneus (20), first (21) and fifth (22) metatarsal heads, and additional markers rigidly attached to a wand over the mid-femurs (15) and mid-shaft of the tibia (18), for both legs. Before trials, a static calibration procedure was carried out for every subject placing 7 additional markers on T10 vertebrae (A), for the upper body; medial epicondyle of the humeri (B), for both arms; medial epicondyle of the femurs (C) and medial malleolus (D), for both legs. **C:** Illustration of the 10 types of perturbations. Each perturbation involved the combination of longitudinal (i.e., North, N or South, S; on the top and on the bottom the respective velocity profiles are reported) and transversal (i.e., East, E, or West, W; on the right the medio-lateral velocity profile is reported) movements of the belt provided while participants were walking at speed v . Five perturbations were delivered on the left foot (i.e., NL, NW, W, SW, SL) and five on the right foot (i.e., NR, NE, E, SE, SR). On the right-top edge of the platform plan, the direction of X, Y and Z axis related to the XYZ right-hand global reference frame are reported. Noticeably, the centre of the reference frame was located in the centre of the platform.

Methods), due to the intrinsic anisotropy of both compliance and inertia of the musculo-skeletal system. If confirmed, these evidences would suggest that whole body reactive response may result from the flexible combination of the same motor schemes involving, at the same time, upper and lower body segments.

II. MATERIALS AND METHODS

A. Participants and Experimental setup

Fifteen healthy adults (10 males and 5 females, 26.1 ± 1.3 years old, 68.8 ± 12.3 kg, 1.78 ± 0.06 m, right dominance of the lower limb) were enrolled for the study after determining lower limb dominance by observing the leg they preferred to use to kick a ball [16]. They were informed about the research procedures before giving their informed consent. Research procedures were in accordance with the Declaration of Helsinki and were approved by the Local Ethical Committee.

Experimental sessions were carried out using SENLY (Figure 1A), a mechatronic platform mainly consisting of two parallel and adjacent treadmills [17]. The treadmills have belts that can be independently moved both longitudinally and transversally (i.e., the right belt can be moved in all clockwise directions from north to south, and the left belt can be moved toward all directions in the remaining hemi-plane) and are wrapped around two platforms provided with force cells. It is possible, in this way, to apply slipping perturbations toward all directions in the horizontal plane by means of sudden movements of one or both treadmills, while measuring the vertical component of the ground reaction forces.

The 3D kinematics of the whole body was recorded using a 6-camera based Vicon 512 Motion Analysis System (Oxford, UK), with sample rate of 100 Hz. A set of 39 spherical markers (14 mm diameter) was located on suitable body landmarks (Figure 1B). A static calibration procedure was carried out

before the trials for each subject by placing 7 additional markers (Figure 1B) used as virtual points to define joint centers of rotation (see *Data Processing*). The 3D kinematics and the ground reaction forces were synchronized by means of a logic pulse generated by SENLY while delivering perturbations.

The global reference frame was located in the centre of SENLY with X axis along the anterior/posterior (AP) direction, Y axis vertical (V), and Z axis defined by the right-hand rule along the medial/lateral (ML) direction (Figure 1C).

B. Protocol

The protocol accounted for 10 perturbations (Figure 1C), which were provided twice for each subject while walking at constant speed, and started when the left or the right heel strike was detected by SENLY. The perturbations were delivered toward several directions, in order to mimic the fact that perturbations leading to accidents can occur in an unlimited number of directions [18], each involving specific muscle recruitment [3].

All perturbations characterized by pure AP belt movements (i.e., NL, NR, SL, SR; Figure 1C) imposed a trapezoidal speed profile to a belt, in which maximum speed (1.88 m/s), acceleration/deceleration (6.65 m/s^2), hold time (0.20 s) and fall time (0.28 s) were fixed. For pure ML perturbations (i.e., W and E; Figure 1C), each belt underwent a triangular speed profile in which acceleration/deceleration (2.40 m/s^2) and rise/fall time (0.25 s) were fixed. For perturbations characterized by the combination of AP and ML belt movements (i.e., NW, SW, NE, SE; Figure 1C), the speed profile consisted of the combination of pure AP and ML movements. Noticeably, each perturbation was delivered either to the left (NL, NW, W, SW, SL) or to the right (NR, NE, E, SE, SR) foot. Ten further trials, in which no perturbation was

applied, were also included in the experimental protocol.

In order to obtain unbiased results: (i) participants did not know whether they would be perturbed or not; (ii) perturbations were supplied in random order; (iii) neither data referring to all second perturbing occurrences, nor data recorded during unperturbed trials were adopted for data analysis.

The baseline walking speed for each subject was chosen in accordance with the principle of dynamic similarity described by the Froude number (F_r) [19]. Specifically, for each subject, the walking speed (v) was calculated by means of the following equation:

$$v = \sqrt{F_r \cdot g \cdot L} \quad (1)$$

where g is the gravitational acceleration (i.e., 9.81 m/s^2) and L is the leg length from the prominence of the greater trochanter external surface to the lateral malleolus. In this study $F_r = 0.15$ was chosen, and a 10 minutes long period was adopted for acclimation. Each recording session began while a subject was walking steadily, started 1 minute before delivering the perturbation in order to include at least five consecutive strides, and finished after the subject recovered balance. Subjects wore a safety harness attached to an overhead track.

C. Data Processing

A full body model accounting for 15 segments and 42 internal degrees of freedom was developed. The 15 segments were: head/neck (H), chest (T), abdomen/pelvis (P), upper arms (LA and RA), forearms (LFA and RFA), hands (LH and RH), thighs (LT and RT), shanks (LS and RS) and feet (LF and RF). All joints were approximated as spherical and their centre was located in accordance with literature [20-23]. For the i^{th} body segment, a right-handed local reference frame was located in its own centre of mass. The X_i axis was oriented toward forward, the Y_i axis was oriented from the distal to the

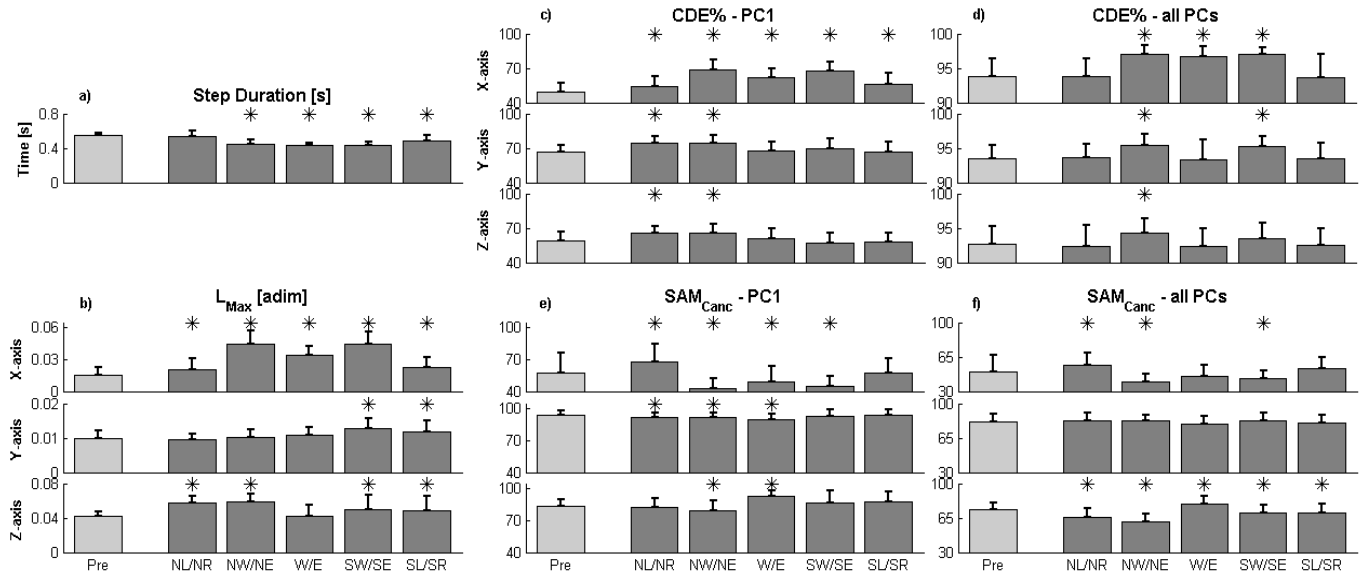


Fig. 2. The subplots show mean and standard deviation (one side error bar) of: a) the step duration; b) the L_{Max} ; c) and d) the CDE% respectively accounting for both PC1 (CDE% - PC1) and all retained components (CDE% - all PCs); e) and f) the SAM_{Canc} respectively accounting for both PC1 (SAM_{Canc} - PC1) and all retained components (SAM_{Canc} - all PCs). The ticks on the horizontal axis for all subplots represent data pre (PRE; light gray) and post (pooled NL/NR, NW/NE, W/E, SW/SE, and SL/SR; dark gray) perturbation. The label * on the top of each bar indicates a significant difference ($p < 0.05$) between data pre and post perturbation.

proximal joint, and the Z_i axis was defined by the right-hand rule.

Body segment inertial parameters (i.e., mass, centre of mass position and moment of inertia tensor) were calculated using procedures described by Zatsiorsky and colleagues [24], and modified by de Leva [25].

Missed kinematic data were estimated by means of cubic spline interpolations. High-frequency related noise was removed from digitized coordinates by low-pass filtering data (zero-lag, 4th order Butterworth low-pass filter) with cut off at 10 Hz. The cut off frequency was selected by means of the procedure described by Winter [26].

Body model and kinematics were used to estimate the SAM of each segment with respect to the whole body's centre of mass, as previously described [12]. Then, the WBAM was calculated as the sum of individual SAMs. WBAM and SAMs were normalized by dividing them by the product of the subject's mass, height, and walking speed [13, 14]. For each subject and each trial, the three components of WBAM (L_{x}^{WB} , L_{y}^{WB} , and L_{z}^{WB}) and SAMs (L_{x}^i , L_{y}^i , and L_{z}^i , where i refers to the i^{th} body segment) were subdivided into two subsets: data recorded before and after the onset of the perturbation. The former referred to the last five ipsilateral unperturbed steps, in

which each cycle started with the heel strike of the leg being perturbed and finished with the heel strike of the contralateral one. These data were subdivided into steps, individually time-interpolated over 101 points, and averaged in order to have a representative step cycle. Data recorded after the onset of the perturbation referred to the compensatory step, in which each cycle started simultaneously with the onset of the perturbation and finished with the landing (i.e., the heel strike) of the unperturbed leg. Data related to the compensatory step were also time-interpolated over 101 points. This procedure provided: two 101x3 matrices describing the WBAM before and after the perturbation; six 101x15 matrices describing the SAM of all body segments, each referring to one of the three axes and related to both the step and the compensatory cycles.

For each subject, the Principal Component Analysis (PCA) was performed on the SAM matrices after standardization with zero mean and unit variance. Retained Principal Components (PCs) were chosen in accordance with the eigenvalue > 1 criterion, and were pooled across subjects by means of the greatest similarity estimated by the cosine of the angle between the unit vectors of the weighting coefficient vectors. Herein, we will adopt the term "homologous" to refer to pooled PCs. Finally, retained PCs were used to estimate the coefficient of SAM cancellation (SAM_{Canc}), as previously described [12].

D. Statistical analysis

The effect of direction of the perturbation (i.e., paired NL/NR, NW/NE, W/E, SW/SE, and SL/SR) and side (i.e., left and right foot) on duration of the compensatory cycle, maximum of the absolute value of L_{x}^{WB} , L_{y}^{WB} , and L_{z}^{WB} (L_{Max}), Cumulative Data Explained (CDE%) and the SAM_{Canc} , accounting for both all retained PCs and only PC1, was analyzed using the two-way ANalysis Of VAriance (ANOVA). Since no significant effect of the side (i.e., right and left feet) was ever observed (see Results, Table I), homologous data related to left and right perturbations were pooled. Then, for each direction, the t-Test was used to compare the same metrics post-perturbation to those referring to the baseline.

In order to define a synthetic measure of the degree of similarity between two PCs, we adopted the absolute value of the Pearson correlation coefficient (ρ) of their weightings. In particular, ρ was used to investigate the association between homologous PCs pre and post perturbation (e.g., ρ_{PC1} , ρ_{PC2} , ρ_{PC3} and ρ_{PC4}). The effect of direction (i.e., paired NL/NR, NW/NE, W/E, SW/SE, and SL/SR) and side (i.e., left and right foot) on ρ was investigated using the two-way ANOVA.

Data analysis was carried out off-line by means of customized MATLAB (The MathWorks Inc., Cambridge, MA, US) scripts, and the statistical significance was set at $p < 0.05$.

III. RESULTS

Subjects walked at an average speed of 1.10 ± 0.03 m/s (range: 1.02-1.14 m/s) and the step cycle was 0.54 ± 0.03 s long. After the perturbation, all participants were able to recover their balance without falling. The compensatory cycle

TABLE I

Metric	Axis	Factor1:	Factor2:
		Side	Direction
Duration of the compensatory step		0.475	<0.001
L_{Max}	X	0.933	<0.001
	Y	0.600	<0.001
	Z	0.223	<0.001
CDE% - PC1	X	0.234	<0.001
	Y	0.774	<0.001
	Z	0.426	<0.001
CDE% - all PCs	X	0.209	<0.001
	Y	0.900	0.001
	Z	0.952	0.043
SAM_{Canc} - PC1	X	0.178	<0.001
	Y	0.855	0.132
	Z	0.574	<0.001
SAM_{Canc} - all PCs	X	0.163	<0.001
	Y	0.384	0.245
	Z	0.085	<0.001
ρ_{PC1}	X	0.001	0.008
	Y	0.028	<0.001
	Z	0.003	0.009
ρ_{PC2}	X	0.092	0.007
	Y	0.073	0.013
	Z	0.171	<0.001
ρ_{PC3}	X	0.174	0.737
	Y	0.201	0.347
	Z	0.058	0.053
ρ_{PC4}	X	0.575	0.538

The table shows the p-values related to the two-way ANOVA for the analysis of the side (i.e., left and right foot) and the direction of the perturbation (i.e., paired NL/NR, NW/NE, W/E, SW/SE, and SL/SR) on reported metrics. When the p-value is statistically significant ($p < 0.05$), it is highlighted in bold.

was 0.46 ± 0.07 s long, about 0.1 s shorter than the unperturbed step ($p < 0.05$ for all directions except for NL/NR; see Figure 2a).

The two-way ANOVA revealed that the duration of the compensatory cycle was significantly ($p < 0.05$) affected by the direction of the perturbation whereas there was no effect of the side (Table I).

A. Whole Body Angular Momentum

Normalized WBAM patterns related to unperturbed steps (Figure 3) were in agreement with previous literature [12-14, 27]. Throughout the step cycle, L_{Max} was 0.016 ± 0.006 , 0.010 ± 0.002 , and 0.042 ± 0.005 respectively for the X, Y, and Z axes (Figures 2b and 3).

During the compensatory step, L_{Max} increased (Figure 2b) and the variability of the WBAM grew from the onset throughout the time window (Figure 3). Noticeably:

- transversal perturbations (i.e., NW, NE, W, E, SW, SE) induced greater variations of L_{x}^{WB} ;
- backward perturbations (i.e., SW, SE, SL, SR) induced greater variations of L_{y}^{WB} ;
- forward perturbations (i.e., NL, NW, NR, NE) induced greater variations of L_{z}^{WB} .

As expected, L_{x}^{WB} and L_{y}^{WB} showed anti-symmetric patterns with respect to the side, whereas L_{z}^{WB} patterns did not differ between sides due to their cyclic features (Figure 3).

B. Segmental Angular Momenta

With respect to the unperturbed step, 4 PCs were retained for the SAMs related to the X axis, and 3 PCs were retained for Y and Z axes. These respectively explained $93.82 \pm 2.55\%$, $93.46 \pm 1.96\%$ and $92.67 \pm 2.64\%$ of the whole data information (Figure 2d). Noticeably, PC1 explained the greatest amount of data variance for all axes ($49.67 \pm 7.55\%$, $66.84 \pm 5.10\%$, and $59.28 \pm 7.11\%$ respectively for the X, Y, and Z axes; see Figure 2c). Moreover, weight coefficients related to PC1, especially Y and Z axes, were more similar across all subjects (as expected [12]) than those referring to the remaining components (Figures 4a, 4b, 4c).

On the whole, with respect to PC1:

- the X axis (see Figure 4a) was mainly loaded by the in-

phase contribution of all body segments, except those of pelvi (P), both thighs (LT and RT) and distal segments of the contralateral arm (LH and LFA);

- the Y and Z axes were characterized by the expected anti-phase relationship between respectively, upper and lower body segments (Figure 4b), and right and left body segments (Figure 4c); moreover, for the Z component, the foot segment ipsilateral to the side of the step cycle was negligible (Figure 4c).

Concerning the other retained PCs:

- for the X axis, only the PC2 accounted for an anti-phase contribution of upper and lower limbs (Figure 4d), whereas body segments did not significantly contribute to PC3 and PC4 (Figures 4g and 4l);
- for the Y axis, we observed the anti-phase relationship between right and left lower body segments and the contribution of P, T, and H to PC2 (Figure 4e); PC3 was instead characterized by very variable weight coefficients (Figure 4h);
- for the Z axis, PC2 showed a significant contribution of many body segments; in particular, we observed that weighting coefficients related to proximal segments appeared in anti-phase with respect to distal ones (Figure 4f); PC3 showed greater variability (Figure 4i).

SAM_{Canc} estimated by all retained PCs was on average $49.65 \pm 16.83\%$, $81.31 \pm 8.16\%$ and $74.01 \pm 6.18\%$, respectively for X, Y and Z axes (Figure 2f) whereas SAM_{Canc} estimated only by the first PC was on average $57.10 \pm 19.57\%$, $94.07 \pm 4.56\%$ and $83.68 \pm 6.28\%$, respectively for X, Y and Z axes (Figure 2e). The AP direction (X axis) was characterized by the lowest values of SAM_{Canc} , in agreement with to previous authors [12].

With respect to the compensatory step, 3 PCs were retained for both Y and Z axes. Conversely, although the eigenvalue > 1 criterion indicated that only 3 PCs were enough to describe data variability related to the X axis, we decided to retain 4 PCs in order to allow comparisons between data sets estimated pre and post perturbation. Accordingly, accounted PCs explained, on average, $95.69 \pm 2.63\%$, $94.21 \pm 2.28\%$ and $92.99 \pm 2.64\%$ of the whole data variance for, respectively, X, Y, and Z axes (Figure 2d). Noticeably, the CDE% increased

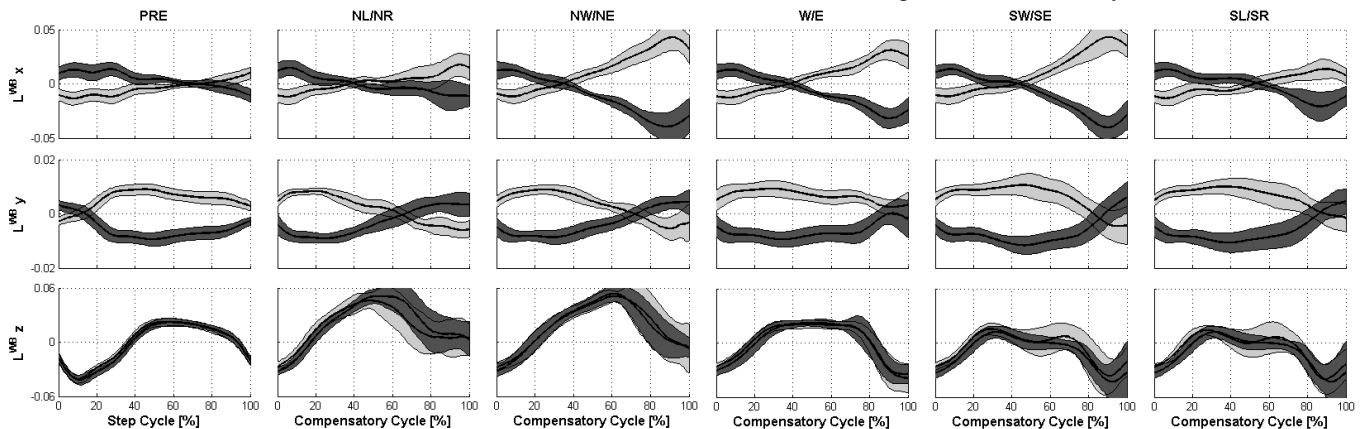


Fig. 3. The figure shows mean and 1 standard deviation (error band) of L_{x}^{WB} , L_{y}^{WB} , and L_{z}^{WB} patterns before (PRE) and after (NL/NR, NW/NE, W/E, SW/SW, SL/SR) perturbation. Specifically, each subplot reports data related to the left (light grey) and right (dark grey) sides.

during the perturbation and that related to the X axis showed the greatest pre versus post deviation (Figure 2d) mainly due to a significant incremental contribution of PC1. On average PC1 explained $61.58 \pm 10.44\%$, $70.63 \pm 8.24\%$ and $61.35 \pm 8.93\%$ of the whole data variance for, respectively, X, Y, and Z axes (Figure 2c).

The PC1 related to all axes was the most consistent component across subjects, and the distribution of its weighting coefficients was comparable among directions (see Figures 4a, 4b and 4c), while the distribution of weight

coefficients of PC2 appeared to depend on the direction of the perturbation (see Figures 4d, 4e and 4f). Weight coefficients related to PC3 and PC4 assumed spread values across perturbations, which did not allow the identification of any univocal behavior (Figure 4).

Although PC1 during the perturbation quite resembled that observed for the unperturbed step, the contribution of some body segments showed specific features. In particular, with respect to the side of perturbation, weight coefficients of the ipsilateral lower body segments (see RF, RS and RT in Figure

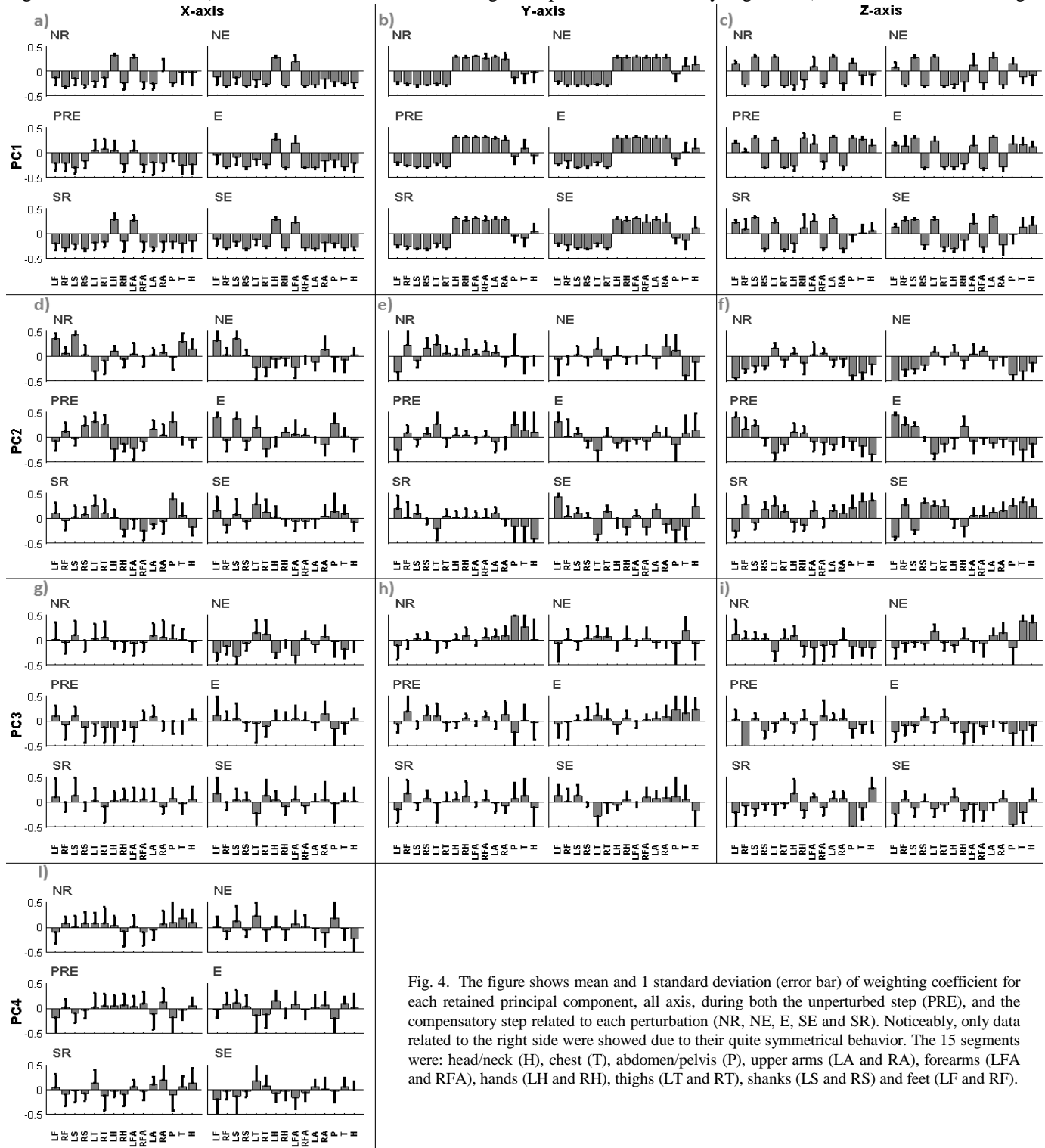


Fig. 4. The figure shows mean and 1 standard deviation (error bar) of weighting coefficient for each retained principal component, all axis, during both the unperturbed step (PRE), and the compensatory step related to each perturbation (NR, NE, E, SE and SR). Noticeably, only data related to the right side were showed due to their quite symmetrical behavior. The 15 segments were: head/neck (H), chest (T), abdomen/pelvis (P), upper arms (LA and RA), forearms (LFA and RFA), hands (LH and RH), thighs (LT and RT), shanks (LS and RS) and feet (LF and RF).

4a) and contralateral upper body segments (see LH, LFA and LA in Figure 4a), related to the X axis, increased and were characterized by a lower inter-subject variability. Regarding the Z axis, we observed an increase in activity of the perturbed foot (see RF in Figure 4c) and a decrease in activity of the trunk segments (see P, T and H in Figure 4c). Moreover, the weight of some body segments (see RF, RH, T and H in Figure 4c) was systematically modulated from negative to positive values in accordance with the direction of the perturbation.

Concerning PC2, the perturbations mainly emphasized the contribution of the contralateral leg segments along the X axis (Figure 4d). Above all, with respect to the Z axis, the sign of the weight coefficients of either the upper or lower limb segments changed with the direction of the perturbation (Figure 4f).

Results reported in Figure 2d and 2f show that SAM_{Canc} related to the X and Z axes ranged across a wide interval than that related to the Y axis, and the minimum values occurred when perturbations were delivered to diagonal directions. Moreover, the SAM_{Canc} did not show a monotonic pre versus post trend (Figures 2e and 2f).

Results also highlighted a certain relationship between the SAM_{Canc} and the L_{Max} mainly for the X and Z axes: when the perturbation involved greater variations of WBAM, the SAM_{Canc} decreased (Figures 2e and 2f). This relationship was expected because, when paired body segments provide in-phase contributions to the WBAM, the WBAM increases, weight coefficients related to such body segments assume the same sign, and the SAM_{Canc} consequently decreases.

The two-way ANOVA (Table I) revealed that, for all components, L_{Max} , CDE%, and SAM_{Canc} were generally not affected ($p > 0.05$) by the side (i.e., left and right), but were influenced by the direction of the perturbation (i.e., paired NL/NR, NW/NE, W/E, SW/SE, and SL/SR). For this reason, data related to homologous perturbations delivered toward the right and the left sides were pooled and compared to those related to unperturbed locomotion. The only exception was SAM_{Canc} related to the Y axis that was not affected by the direction either (Table I).

C. Comparison between unperturbed and perturbed angular momentum

Figure 5 shows the degree of association between homologous PCs pre and post perturbation, and highlights that:

- ρ_{PC1} was characterized by high values above all with respect to the Y (0.88 ± 0.08) and the Z axes (0.69 ± 0.13); instead, it assumed lower values (0.47 ± 0.27) for the X axis, mainly due to perturbations delivered toward the north direction;
- ρ_{PC2} related to the Y and the Z axes was directionally tuned; perturbations involving movements of the belts toward the backward and/or lateral sides showed greater similarity with data related to locomotion; the comparison related to the X axis showed greater variability even though values increased when perturbations accounted for longitudinal movements of

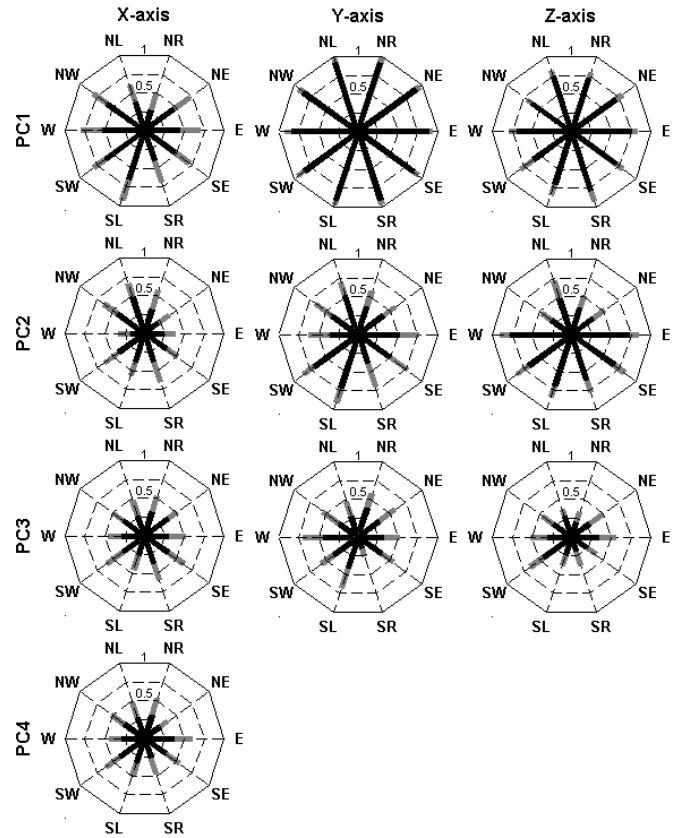


Fig. 5. The figure shows the Pearson correlation coefficient (ρ) of weighting coefficients related to the unperturbed step and the compensatory step toward all directions. Black and grey bars respectively represent mean values and one standard deviation.

the belts;

- ρ_{PC3} and ρ_{PC4} were always characterized by a significant variability among subjects (see also Figure 4), which did not allow the identification of any univocal behavior.

The two-way ANOVA (Table I) revealed that the direction of the perturbation (i.e., paired NL/NR, NW/NE, W/E, SW/SE, and SL/SR) for all axes significantly affected ($p < 0.05$) the similarity of the weight coefficient related to PC1 and PC2 between pre and post perturbation (ρ_{PC1} and ρ_{PC2}). Instead, the side of the perturbation (i.e., right and left foot) only influenced ρ_{PC1} , for all axes. In particular, ρ_{PC1} related to the X axis was greater on the left side, while those referring to the Y and Z axes were slightly greater on the right side (Figure 5).

IV. DISCUSSION

This paper aimed at investigating the main rules underlying the contribution of all body segments while keeping balance in response to unexpected and multidirectional slipping perturbations, by analyzing WBAM and SAM variations. Specifically, we investigated the hypothesis that whole body response is characterized by similar features while both walking and keeping balance due to an unexpected perturbation, thus highlighting that the movement of upper and lower body segments always results from the flexible combination of the same motor schemes.

To the best of our knowledge, this is the first work that extends the traditional approach, based on mono-directional

AP perturbations of a single foot during walking, to a standardized paradigm accounting for multi-directional perturbations applied to both feet, one at a time. Indeed, although many research groups have studied the effects of multidirectional perturbations during standing [18, 28-30], only Oddsson and colleagues investigated balance control after perturbations provided on the right foot toward two diagonal directions while walking [31].

A. Consistence of retained components

The main hypothesis underlying SAM decomposition is that inter-limb coordination is characterized by a significant degree of co-variation of all L's, such that their modulation is constrained in order to achieve a dimensional reduction of the complexity related to balance control. Our results (see Figures 2 and 4) widely confirm this hypothesis during both the unperturbed and perturbed step cycles.

The eigenvalue >1 criterion allowed to retain the same number of components of previous authors [12], capturing over 90% of data variability of the SAM estimated during the unperturbed steps, for all axes. Nevertheless, results (see Figures 2 and 4) showed that PC1 and PC2, for all axes, were comparable to those previously reported [12-14] and more consistent across subjects, whereas the other PCs were characterized by greater inter-subject variability.

One of the critical points of the PCA is that, although retained PCs represent the threshold between capturing random fluctuations and systematic behavior, those accounting for lower variance (e.g., PC3 and PC4 in our case) are usually characterized by greater inter-subject variability, such that they do not provide any univocal and functional description across all datasets. This behavior has also been noticed by previous authors who have dealt with SAM decomposition [13, 14] or analyzed other types of datasets [29, 32].

Indeed, despite the fact that retained PCs accounting for lower variance can provide a measure of coordination variability [33], or can highlight the subtle effects of the experimental manipulations (e.g., the influence of walking speed on the activity of a single muscle; see [34]), the functional description of the less significant PCs over the whole group of subjects still remains an open question. Therefore, with respect to our study, we believe that the main features underlying SAM coupling among body segments, which were commonly relevant across all participants, were only described by PC1 and PC2.

B. Effects of the side of the perturbation on WBAM and SAM decomposition

Results (Table I) showed that all adopted metrics describing the overall kinematics and dynamics of the perturbed step (i.e., L_{Max} , SAM_{Canc} , $CDE\%$, and duration of the Compensatory Cycle) were not affected by the side (i.e., left or right foot) of the delivered perturbation. Conversely, ρ_{PC1} was significantly ($p<0.05$; see Table I and Figure 5) affected by it. Specifically: with respect to the X axis, perturbations delivered toward the left side were those characterized by the greatest ρ ; with

respect to the Y and the Z axes, perturbations delivered toward the right side were those characterized by the greatest ρ . Moreover, the difference between the sides was more marked on the X axis (Figure 5).

On the one hand, these results suggest that the overall angular momentum generated by the compensative reaction of all body segments working together does not depend on the dominance of the subject; that is, perturbations delivered to the left and the right sides were sufficiently symmetric for subjects to recover balance using a mirrored WBAM. On the other hand, overall motor outcome was obtained by differently coupling body segments with respect to the side of the perturbation, revealing an asymmetric inter-limb coordination behavior.

The presence of symmetry and asymmetry during unperturbed walking has been widely debated in literature. In particular, the coordinated movement of arms and legs is not expected to depend on the side since resulting from the oscillating activity of coupled motoneuronal pools each leading a hemi-portion of both the upper and the lower musculo-skeletal system [8, 35, 36]. Nevertheless, some studies have evidenced that, during walking, the non-dominant leg is mainly responsible for support and body weight transfer while the contralateral one contributes more to propulsion [37, 38]. Accordingly, other authors observed an asymmetric behavior of the ground reaction force reflecting a different approach between the sides while controlling medio-lateral balance [39].

Results showed that the X axis was markedly influenced by the laterality of the perturbation such that those delivered toward the non-dominant side increased ρ (Figure 5). This suggests that the non-dominant leg is able to manage support and control functions by adopting motor schemes, which have been strongly trained during walking. Conversely, a perturbation delivered toward the dominant limb elicits motor outcomes reflecting participant-related variation of control strategies because it is mainly responsible for propelling forward the body.

Indeed, although we would have expected the decomposition of all SAM components to be characterized by the same behavior (e.g., ρ related to the left side should have been greater than that referring to the right one for all axes), this did not occur (Figure 5). However, it is important to underline that the difference of ρ between the sides relating to the Y and Z axes was small (Figure 5), and inter-limb coordination in the frontal plane (e.g., X axis) was markedly strengthened due to the perturbation (Figure 2c). Therefore, we believe that the behavior of ρ related to the Y and Z axes was subordinated to balance control in the frontal plane (X axis), which requires greater effort by the CNS because it is more inherently unstable [40].

To the best of our knowledge, reported results have never been observed in literature probably because unexpected multi-directional perturbations during quite upright stance have always been delivered on both feet (i.e., they are bilateral tasks; see [28-30, 41]), that is, a different approach between the limbs

is not required. In our protocol, instead, the role of the lower limbs while managing perturbations was different: the perturbed leg was initially asked to control interaction with the treadmill while the contralateral leg was mainly extended to achieve greater stability as soon as possible.

To conclude, results suggest that the observed asymmetrical behavior may result from multifactorial reasons mainly related to the dominance of participants. However, further investigations aimed at deeply analyzing the effect of the dominance on the motor schemes elicited during multidirectional perturbations will be carried out to confirm or less our hypothesis.

C. Effects of the direction of the perturbation on WBAM and SAM decomposition

As expected, the direction of the perturbation (i.e., paired NL/NR, NW/NE, W/E, SW/SE, and SL/SR) significantly affected metrics related to kinematics and dynamics of the compensatory step (i.e., L_{Max} , SAM_{Canc} , CDE%, and the duration of the Compensatory Cycle), and ρ related to PC1 and PC2 (see Figure 5 and Table I). In particular, since adequate balance corrections in two planes may be more destabilizing [30], perturbations characterized by the diagonal movement of the belt (NE/NW and SE/SW) involved the greatest increase in L_{Max} and CDE%, and decrease in SAM_{Canc} (Figure 2). This hence suggests that body segments contribute cumulatively to generate a counteracting variation of the WBAM able to suitably compensate the most destabilizing perturbations.

Furthermore, weight coefficients of both PC1 and, more evidently, PC2 appeared directionally tuned (see Figures 4 and 5, and Table I), highlighting an AP axis of symmetry of ρ (Figure 5).

On the whole, this behavior most likely resulted from the different kinematic features of perturbations involving distinct biomechanical affordances and demands, and reflected the anisotropy of anatomical restrictions and passive properties (e.g., stiffness, inertia) of the musculo-skeletal system. Moreover, it confirms that the CNS is able to rapidly interpret multiple sensory input signals from all body segments, in order to produce context-dependent motor schemes leading to suitable regulation of the angular momentum and recovery of balance.

D. Inter-limb coordination

The effect of the perturbation on the WBAM generated an increase in L_{Max} (Figures 2b and 3) and a positive deviation of CDE%, above all for the PC1 (Figure 2c), revealing that the contribution of all body segments co-varied more consistently than during locomotion. As expected, body segment coupling due to the lack of balance did not keep the WBAM as close to zero as during walking (Figures 2b and 3), in accordance with the evidence that certain motor tasks (e.g., see skaters while spinning) must be carried out only with a consistent generation of angular momentum [12]. In this regard, WBAM modulation appears as a mechanism that leads balance regulation by properly organizing the co-variation of elemental variables

[42].

The significant growth of the CDE% reveals that motor patterns subjected to the control of equilibrium during reactive control (e.g., as while managing unexpected perturbations) are more consistent across segments than those used during proactive control (e.g., as while walking), despite the many options available [43]. Moreover, it corroborates the hypothesis that the WBAM can be considered as a controlled variable of the CNS [12, 13] resulting from a coordinated grouping of SAMs even during unusual motor tasks.

A similar behavior of CDE% was also observed by Bennett and colleagues [14] who reported that the variance described by the retained components related to the Y and Z axes increased with the increase in walking speed. Noticeably, our results showed that the CDE% significantly increased for all axes, but the greatest growth occurred with respect to the X axis (Figure 2c).

All these evidences suggest that when the dynamical stability of a motor task is challenged (e.g., from walking to running or from walking to managing unexpected perturbations), the CNS appears to constraint the coordination of body segments with more rigid schemes, with the aim to suitably control the WBAM. With respect to our study, since segment coupling was more strengthened in the frontal plane than in the others, results confirm that balance regulation due to lateral instability requires further active efforts in order to avoid falling [12, 40]. In this regard, the coupling between perturbed leg and contralateral arm (Figure 4a), as also observed by other authors [9, 11], document that the coordination of upper and lower body segments is synergistically achieved also while managing perturbations, and support the hypothesis that movement control may be led by neural pathways connecting the upper and lower motoneuronal pools of the spinal cord [15].

V. CONCLUSIONS

This study highlighted that the inter-segment coupling underlying whole body response during multi-directional perturbations has features similar to locomotion. However, reactive response to the perturbations elicits motor schemes more consistent across segments than during walking. This behavior is marked in the frontal plane that involves most inherently unstable balance control.

Results also pinpointed the distinct biomechanical affordance and demand of the neuro-musculo-skeletal system, due to both the direction and the side of the perturbation, documenting the attitude of the CNS to interpret multiple sensory inputs in order to produce context-dependent reactive responses. In this respect, further investigations are required in order to deeply analyze the influence of dominance on elicited motor schemes.

Finally, our results confirm that the coordination of upper and lower body segments is synergistically achieved, strengthening the hypothesis that it may result from common neural pathways [8, 10, 15].

REFERENCES

- [1] M. H. van der Linden, D. S. Marigold, F. J. Gabreels, and J. Duysens, "Muscle reflexes and synergies triggered by an unexpected support surface height during walking," *J Neurophysiol*, vol. 97, pp. 3639-50, May 2007.
- [2] D. S. Marigold and A. E. Patla, "Adapting locomotion to different surface compliances: neuromuscular responses and changes in movement dynamics," *J Neurophysiol*, vol. 94, pp. 1733-50, Sep 2005.
- [3] P. F. Tang, M. H. Woollacott, and R. K. Chong, "Control of reactive balance adjustments in perturbed human walking: roles of proximal and distal postural muscle activity," *Exp Brain Res*, vol. 119, pp. 141-52, Mar 1998.
- [4] B. E. Moyer, M. S. Redfern, and R. Cham, "Biomechanics of trailing leg response to slipping - evidence of interlimb and intralimb coordination," *Gait Posture*, vol. 29, pp. 565-70, Jun 2009.
- [5] D. S. Marigold, A. J. Bethune, and A. E. Patla, "Role of the unperturbed limb and arms in the reactive recovery response to an unexpected slip during locomotion," *J Neurophysiol*, vol. 89, pp. 1727-37, Apr 2003.
- [6] M. Pijnappels, M. F. Bobbert, and J. H. van Dieen, "Contribution of the support limb in control of angular momentum after tripping," *J Biomech*, vol. 37, pp. 1811-8, Dec 2004.
- [7] J. J. Eng, D. A. Winter, and A. E. Patla, "Strategies for recovery from a trip in early and late swing during human walking," *Exp Brain Res*, vol. 102, pp. 339-49, 1994.
- [8] V. Dietz, K. Fouad, and C. M. Bastiaanse, "Neuronal coordination of arm and leg movements during human locomotion," *Eur J Neurosci*, vol. 14, pp. 1906-14, Dec 2001.
- [9] M. Pijnappels, I. Kingma, D. Wezenberg, G. Reurink, and J. H. van Dieen, "Armed against falls: the contribution of arm movements to balance recovery after tripping," *Exp Brain Res*, vol. 201, pp. 689-99, Apr 2010.
- [10] D. S. Marigold and J. E. Misiaszek, "Whole-body responses: neural control and implications for rehabilitation and fall prevention," *Neuroscientist*, vol. 15, pp. 36-46, Feb 2009.
- [11] P. E. Roos, M. P. McGuigan, D. G. Kerwin, and G. Trewartha, "The role of arm movement in early trip recovery in younger and older adults," *Gait Posture*, vol. 27, pp. 352-6, Feb 2008.
- [12] H. Herr and M. Popovic, "Angular momentum in human walking," *J Exp Biol*, vol. 211, pp. 467-81, Feb 2008.
- [13] T. Robert, B. C. Bennett, S. D. Russell, C. A. Zirker, and M. F. Abel, "Angular momentum synergies during walking," *Exp Brain Res*, vol. 197, pp. 185-97, Aug 2009.
- [14] B. C. Bennett, S. D. Russell, P. Sheth, and M. F. Abel, "Angular momentum of walking at different speeds," *Hum Mov Sci*, vol. 29, pp. 114-24, Feb 2010.
- [15] V. Dietz, "Do human bipeds use quadrupedal coordination?," *Trends Neurosci*, vol. 25, pp. 462-7, Sep 2002.
- [16] S. Coren and C. Porac, "The validity and reliability of self-report items for the measurement of lateral preference," *British Journal of Psychology*, vol. 69, p. 5, 1978.
- [17] L. Bassi Luciani, V. Genovese, V. Monaco, L. Odetti, E. Cattin, and S. Micera, "Design and Evaluation of a new mechatronic platform for assessment and prevention of fall risks," *J Neuroeng Rehabil*, vol. 9, p. 51, Jul 28 2012.
- [18] B. E. Maki, W. E. McIlroy, and S. D. Perry, "Influence of lateral destabilization on compensatory stepping responses," *J Biomech*, vol. 29, pp. 343-53, Mar 1996.
- [19] C. L. Vaughan and M. J. O'Malley, "Froude and the contribution of naval architecture to our understanding of bipedal locomotion," *Gait Posture*, vol. 21, pp. 350-62, Apr 2005.
- [20] X. Wang, "Construction of arm kinematic linkage from external surface markers," *Proceeding of the 4th International Symposium on 3D Analysis of Human Movement*, 1996.
- [21] C. Anglin and U. P. Wyss, "Arm motion and load analysis of sit-to-stand, stand-to-sit, cane walking and lifting," *Clin Biomech (Bristol, Avon)*, vol. 15, pp. 441-8, Jul 2000.
- [22] A. L. Bell, D. R. Pedersen, and R. A. Brand, "A comparison of the accuracy of several hip center location prediction methods," *J Biomech*, vol. 23, pp. 617-21, 1990.
- [23] R. B. Davis, S. Ounpuu, D. Tyburski, and J. R. Gage, "A gait analysis data collection and reduction technique," *Hum. Mov. Sci.*, vol. 10, pp. 575-587, 1991.
- [24] V. M. Zatsiorsky, V. N. Seluyanov, and L. G. Chugunova, "Methods of determining mass-inertial characteristics of human body segments," *Contemporary Problems of Biomechanics*, pp. 272-291, 1990.
- [25] P. de Leva, "Adjustments to Zatsiorsky-Seluyanov's segment inertia parameters," *J Biomech*, vol. 29, pp. 1223-30, Sep 1996.
- [26] D. A. Winter, *Biomechanics and Motor Control of Human Movement*. New York: John Wiley & Sons, Inc., 1990.
- [27] G. G. Simoneau and D. E. Krebs, "Whole-Body Momentum During Gait: A Preliminary Study of Non-Fallers and Frequent Fallers," *J Appl Biomech*, vol. 16, pp. 1-13, 2000.
- [28] J. H. Allum, M. G. Carpenter, and F. Honegger, "Directional aspects of balance corrections in man," *IEEE Eng Med Biol Mag*, vol. 22, pp. 37-47, Mar-Apr 2003.
- [29] G. Torres-Oviedo and L. H. Ting, "Muscle synergies characterizing human postural responses," *J Neurophysiol*, vol. 98, pp. 2144-2156, Oct 2007.
- [30] J. H. Allum, M. G. Carpenter, F. Honegger, A. L. Adkin, and B. R. Bloem, "Age-dependent variations in the directional sensitivity of balance corrections and compensatory arm movements in man," *J Physiol*, vol. 542, pp. 643-63, Jul 15 2002.
- [31] L. I. Oddsson, C. Wall, M. D. McPartland, D. E. Krebs, and C. A. Tucker, "Recovery from perturbations during paced walking," *Gait Posture*, vol. 19, pp. 24-34, Feb 2004.
- [32] V. Monaco, A. Ghionzoli, and S. Micera, "Age-related modifications of muscle synergies and spinal cord activity during locomotion," *J Neurophysiol*, vol. 104, pp. 2092-102, Oct 2010.
- [33] A. Forner-Cordero, O. Levin, Y. Li, and S. P. Swinnen, "Principal component analysis of complex multijoint coordinative movements," *Biol Cybern*, vol. 93, pp. 63-78, Jul 2005.
- [34] A. Daffertshofer, C. J. Lamoth, O. G. Meijer, and P. J. Beek, "PCA in studying coordination and variability: a tutorial," *Clin Biomech (Bristol, Avon)*, vol. 19, pp. 415-28, May 2004.
- [35] Y. P. Ivanenko, G. Cappellini, N. Dominici, R. E. Poppele, and F. Lacquaniti, "Modular control of limb movements during human locomotion," *J Neurosci*, vol. 27, pp. 11149-61, Oct 10 2007.
- [36] E. P. Zehr and J. Duysens, "Regulation of arm and leg movement during human locomotion," *Neuroscientist*, vol. 10, pp. 347-61, Aug 2004.
- [37] H. Sadeghi, P. Allard, and M. Duhaime, "Functional gait asymmetry in able-bodied subjects," *Hum Mov Sci*, vol. 16, pp. 243-258, 1997.
- [38] H. Sadeghi, P. Allard, F. Prince, and H. Labelle, "Symmetry and limb dominance in able-bodied gait: a review," *Gait Posture*, vol. 12, pp. 34-45, Sep 2000.
- [39] N. Matsusaka, M. Fujitta, A. Hamamina, T. Norimatsu, and R. Suzuki, "Relationship between right and left leg in human gait from a viewpoint of balance control," in *Biomechanics IX-A*, N. R. Winter D.A., Wells R., Hayes K., Patla A., editors, Ed., ed Champaign: Human Kinetics Publishers, 1985, pp. 427-430.
- [40] A. D. Kuo, "Stabilization of lateral motion in passive dynamic walking," *The International Journal of Robotics Research*, vol. 18, p. 14, 1999.
- [41] B. E. Maki and W. E. McIlroy, "Postural control in the older adult," *Clin Geriatr Med*, vol. 12, pp. 635-58, Nov 1996.
- [42] M. L. Latash, "Motor synergies and the equilibrium-point hypothesis," *Motor Control*, vol. 14, pp. 294-322, Jul 2010.
- [43] J. E. Misiaszek, "Neural control of walking balance: if falling then react else continue," *Exerc Sport Sci Rev*, vol. 34, pp. 128-34, Jul 2006.